The current issue and full text archive of this journal is available at
www.emeraldinsight.com/0961-5539.htm

Effect of viscous dissipation on mixed convection flow of water near its density maximum in a rectangular enclosure with isothermal wall

Received September 2003
Revised March 2005
Accepted June 2005

Md. Anwar Hossain
Department of Mathematics, University of Dhaka, Dhaka, Bangladesh, and
Rama Subba Reddy Gorla
Department of Mechanical Engineering, Cleveland State University, Cleveland, Ohio, USA

Abstract

Purpose – To investigate the effect of viscous dissipation on unsteady, combined convective heat transfer to water near its density maximum in a rectangular cavity.

Design/methodology/approach – The upwind finite difference scheme along with successive over relaxation iteration technique is used to solve the governing equations for mixed convection flow of water with density maximum inversion in a rectangular cavity.

Findings – The effect of viscous dissipation was to increase the fluid temperature and resulted in the formation of vortex motion near the lower part of the cavity in an opposite direction to the central vortex. An increase in the Eckert number and Reynolds number of the flow resulted in augmented surface heat transfer rates from the top heated surface.

Research limitations/implication – The analysis is valid for unsteady, two dimensional laminar flow. Isothermal conditions are assumed for the top and bottom walls. An extension to unsteady three dimensional flow case is left for future work.

Practical implications – The method is very useful to analyze nuclear reactor thermal/hydraulic loss of coolant transients, energy conservation, ventilation of rooms, solar energy collection, cooling of electronic equipment, dispersion of waste heat in estuaries and crystal growth in liquids.

Originality/value – The results of this study may be of interest to engineers interested in heat transfer augmentation of mixed convection in window cavities.

Keywords Convection, Fluids, Water, Flow

Paper type Research paper

Nomenclature

C_p	= specific heat at constant pressure ($J\,kg^{-1}\,K^{-1}$)	Gr	= Grashof number
g	= gravitational acceleration (m/sec^2)	H	= enclosure height (m)
Ra	= Rayleigh number	K	= effective thermal conductivity of the media (W/m K)
Re	= Reynolds number	p	= fluid pressure (Pa)

The authors express their gratitude and thank to the reviewers for their valuable comments and suggestions for the improvement of the quality of this piece of work.

International Journal of Numerical Methods for Heat & Fluid Flow
Vol. 16 No. 1, 2006
pp. 5-17

0961-5539
DOI 10.1108/09615530610636928

Pr = Prandtl number
t = time (s)
T = temperature (°C)
u = velocity in x-direction (m/s)
U_0 = velocity of the moving surface
v = velocity in y-direction (m/s)
W = enclosure width (m)
x, y = Cartesian coordinates (m)
X, Y = dimensionless coordinates
β = coefficient of thermal expansion of fluid (K^{-1})
θ = dimensionless temperature
λ = dimensionless heat absorption/generation parameter
μ = effective dynamic viscosity (Pa/s)
ν = effective kinematic viscosity (μ/ρ)
ρ = fluid density at reference temperature (T_c)
τ = dimensionless time
ψ = stream function (m^2/s)
Ω = dimensionless vorticity

1. Introduction

Combined convective heat transfer in cavities has possible applications in many engineering, technological, and natural processes. This includes nuclear reactors, solar ponds, lakes and reservoirs (Imberger and Hamblin, 1982), solar collectors (Ideriah, 1980), and crystal growth (Moallemi and Jang, 1992). Moreover, the flow and heat transfer in a shear- and buoyancy-driven cavity arise in industrial processes such as food processing and float glass production (Pilkington, 1969).

Combined forced-free convective flow in lid-driven cavities or enclosures occurs as a result of two competing mechanisms. The first is due to shear flow caused by the movement of one of the walls of the cavity while the second is due to buoyancy flow produced by thermal non-homogeneity of the cavity boundaries. Understanding of these mechanisms is of great significance from technical and engineering standpoints. This problem has been used extensively as a benchmark case for the evaluation of numerical solution procedures for the Navier-Stokes equations (Agarwal, 1981; Young *et al.*, 1976; Morzynski and Popiel, 1988; Thompson and Ferziger, 1989; Schreiber and Keller, 1983). Koseff and Street (1984) studied experimentally as well as numerically the re-circulation flow patterns for a wide range of Reynolds (*Re*) and Grashof (*Gr*) numbers. Their results showed that the three-dimensional features, such as corner eddies near the end walls, and Taylor-Gortler like longitudinal vortices, have significant effects on the flow patterns for low *Re*.

Both thermally stable and unstable lid-driven flows inside enclosures were investigated numerically by Torrance *et al.* (1972) for fixed values of *Re* and *Pr*. Their numerical results indicated that the Richardson number, which represents the ratio of buoyancy to shear forces, is a controlling parameter for the problem. Prasad and Kose (1989) conducted an experimental investigation of recirculating flow caused by combined forced and natural convection heat transfer in a deep lid-driven cavity filled with water. For the range of the governing parameters studied, their results indicate that the overall heat transfer rate is a very weak function of the *Gr* for the examined range of the *Re*. The effects of the Prandtl number (*Pr*) on laminar mixed convection heat transfer in a lid-driven cavity were studied numerically by Moallemi and Jang (1992). Their numerical simulations revealed that the influence of the thermal buoyancy force on the flow and heat transfer inside cavities is predicted to be more pronounced for higher values of *Pr*. Later, Iwatsu *et al.* (1993) analyzed numerically mixed convection heat transfer in a driven cavity with a stable vertical temperature gradient. Their results showed that the flow features are similar to those of a conventional driven cavity of a non-stratified fluid for small values of the Richardson

number (Ri). Also, it was found that for high values of the Richardson number, much of the fluid in both the middle and bottom portions of the cavity interior is stagnant. Recently, Aydin (1999) investigated aiding and opposing mechanisms of mixed convection in a shear- and buoyancy-driven cavity and determined the range of the Richardson number for the forced-mixed-free convection regimes.

All the above studies were confined to fluids other than water with maximum density inversion. It is well known that studies of the effects of density variation are associated primarily with two topics. The first is Rayleigh-Benard instability that is caused by a negative vertical temperature gradient. At and above a critical Rayleigh number convection develops in the unstable lower layer and extends into the stable upper layer (see Musman, 1968; Merker *et al.*, 1973; Moore and Weiss, 1973; Robillard and Vasseur, 1981). The second is natural convection in an enclosure that is induced by sidewall heating where the two vertical walls are held at different temperatures. In this case, fluid motion occurs at all nonzero values of the Rayleigh number.

Watson (1972) analyzed the effect of density inversion on the fluid flow and heat transfer in a square vessel for values of Ra, the Rayleigh number, which were less than 2×10^4. The results showed that the maximum density effect is greatest when $\Delta T = 8$°C. Seki *et al.* (1978) investigated natural convection both numerically and experimentally in rectangular vessels. The cold vertical wall was maintained at 0°C while the hot wall temperature varied from 1 to 12°C. Lin and Nansteel (1987) investigated numerically the natural convection in a square enclosure containing water near its density maximum and found multi-cellular flow structures for certain ranges of values of the density distribution parameter which is independent of Ra.

In all the above-quoted studies the following parabolic density-temperature relationship (as given by Gebhart and Mollendorf, 1977) was considered:

$$\rho = \rho_0[1 - \beta(T - T_0)^2] \tag{1}$$

where $\beta = 8 \times 10^{-6}$°C^{-2} and ρ_0 is the maximum density which occurs at the temperature $T_0 = 3.98$°C. Tong and Koster (1993) used the above density-temperature relation to investigate natural convection flow of water in a differentially heated rectangular cavity with adiabatic horizontal walls. Such work was extended by Ishikawa *et al.* (2000) whose numerical simulations also took into consideration the temperature dependence of the fluid density, thermal conductivity and viscosity for water near to 4°C as prescribed by the above authors.

Very recently, Hossain and Rees (2003) have investigated convective flow in a cavity which is induced by differential heating of the sidewalls and assisted by internal heating. In this investigation, attention has been focused on convection near the density minimum for water and the Prandtl and Rayleigh numbers have been fixed at $Pr = 11.58$ and $Ra = 10^5$.

Further it should be mentioned that in all the above studies the effect of heat due to viscous dissipation in the flow field and the heat transfer has been neglected. The present work, therefore, extends the previous studies of mixed convection flow of water with density maximum inversion confined in a rectangular cavity by bringing into account the effect of the heat due to viscous dissipation. In this case, we consider the fact that two horizontal surfaces are maintained at two different uniform temperatures and the vertical surfaces are insulated. Further the top horizontal surface is kept moving in its own plane at a constant speed while all other surfaces are fixed.

The reduced dimensionless equations governing the flow have been simulated numerically by employing an upwind finite-difference method, together with the successive over-relaxation (SOR) iteration technique. The results are displayed graphically in terms of streamlines and isotherms, which show the combined effect of heat due to viscous dissipation and density inversion for cavities with differential heating of the horizontal surfaces.

2. Formulation of the problem

Consider a rectangular enclosure of height H and of width W filled with water at maximum density, with top moving surface and bottom surface maintained at a constant temperature T_H and T_C ($T_H > T_C$) and with two insulated vertical walls. In the flow field, we also bring into account the effect of heat due to viscous dissipation. We further assume unsteady laminar flow of a viscous incompressible fluid having constant properties. The effect of buoyancy is included through the well-known Boussinesq approximation. Finally, the direction of the gravitational force is as indicated in Figure 1.

The governing non-dimensional equations, expressing the conservation of mass, momentum, energy are:

$$\nabla \cdot \mathbf{V} = 0 \tag{2}$$

$$\frac{\partial \mathbf{V}}{\partial \tau} + \mathbf{V} \cdot \nabla \mathbf{V} = -\nabla p + \frac{1}{Re} \nabla^2 \mathbf{V} + \frac{Gr}{Re^2} \theta^2 \mathbf{e} \tag{3}$$

$$\frac{\partial \theta}{\partial \tau} + \mathbf{V} \cdot \nabla \theta = \frac{1}{PrRe} \nabla^2 \theta + \frac{Ec}{Re} \Phi \tag{4}$$

where $\mathbf{e} = (0, 1)$ is a unit vector in the direction of the buoyancy force, $\mathbf{V} = \{U, V\}$ is the velocity vector, p is the pressure, θ is the temperature function and Φ is the viscous dissipation function, which is defined by:

$$\Phi = 2\left[\left(\frac{\partial U}{\partial X}\right)^2 + \left(\frac{\partial V}{\partial Y}\right)^2\right] + \left(\frac{\partial U}{\partial Y} + \frac{\partial V}{\partial X}\right)^2 \tag{5}$$

where

$$Re = \frac{U_0 H}{\nu}, \quad Ra = \frac{g\beta(\Delta T)^2 H^3}{\alpha\nu}, \quad Pr = \frac{\nu}{\alpha}, \quad Gr = \frac{Ra}{Pr}, \quad Ec = \frac{U_0^2}{C_p \Delta T} \tag{6}$$

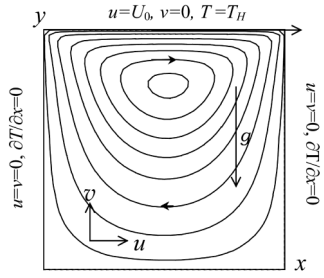

Figure 1.
The flow configuration and the coordinate system

are, respectively, the Reynolds number, Rayleigh number, Prandtl number Grashof number, and the viscous dissipation parameter, known as Eckert number.

The dimensionless variables are given as follows:

$$X = \frac{x}{H}, \quad Y = \frac{y}{H}, \quad \tau = \frac{tU_0}{H}, \quad \mathbf{V} = \frac{\mathbf{v}}{U_0}, \quad \theta = \frac{T - T_0}{\Delta T} \tag{7}$$

where, $\Delta T = T_H - T_C$, $T_0 = (T_H + T_C)/2$ is the mean temperature and $\mathbf{v} = (u, v)$.

Boundary conditions:

$$\begin{aligned} &U = 1, \quad V = 0, \quad \theta = (T_H - T_0)/\Delta T \quad \text{at } Y = 1 \\ &U = 0, \quad V = 0, \quad \theta = (T_C - T_0)/\Delta T \quad \text{at } Y = 0 \\ &\mathbf{V} = 0, \quad \frac{\partial \theta}{\partial Y} = 0 \quad \text{at } X = 0, A \end{aligned} \tag{8}$$

where $A = W/H$ is the dimensionless width of the cavity.

Eliminating the pressure terms from equation (3) and using the equation of continuity (2) gets

$$\frac{\partial \Omega}{\partial t} + \frac{\partial (U\Omega)}{\partial X} + \frac{\partial (V\Omega)}{\partial Y} = \frac{1}{Re}\left(\frac{\partial^2}{\partial X^2} + \frac{\partial^2}{\partial Y^2}\right)\Omega + 2\frac{Gr}{Re^2}\theta\frac{\partial \theta}{\partial X} \tag{9}$$

where

$$\Omega = -\left(\frac{\partial^2}{\partial X^2} + \frac{\partial^2}{\partial Y^2}\right)\psi \tag{10}$$

is the vorticity and ψ is the stream function defined by:

$$U = \frac{\partial \psi}{\partial Y}, \quad V = -\frac{\partial \psi}{\partial X} \tag{11}$$

The energy equation now may, also, be obtained as:

$$\frac{\partial \theta}{\partial t} + \frac{\partial (U\theta)}{\partial X} + \frac{\partial (V\theta)}{\partial Y} = \frac{1}{PrRe}\left(\frac{\partial^2}{\partial X^2} + \frac{\partial^2}{\partial Y^2}\right)\theta + \frac{Ec}{Re}\Phi \tag{12}$$

Knowing the solutions of equations (9)-(12) satisfying the boundary conditions given in (8) one can calculate the rate of heat transfer in terms of the Nusselt number at the left and right walls of the cavity, from the following relation:

$$Nu = -\left(\frac{\partial T}{\partial Y}\right)_{Y=0,1} \tag{13}$$

Solutions of equations (9)-(12) that govern the flow are obtained numerically employing an upwind finite-difference method, together with a SOR iteration technique. Details of this method had already been discussed in Hossain and Wilson (2002) and Hossain and Rees (2003, 2004). It is clear that the non-dimensional parameters of interest are the Reynolds number, *Re*; Grashof number, *Gr*; the Prandtl number, *Pr*; the dissipation parameter, *Ec*. In the present investigation, keeping fixed the values of the Prandtl

number at 11.58 and the Grashof number at 10^5, solutions are obtained for values of $Ec = 0.0$, 0.05, and 0.1 at $Re = 100$. Solutions are also obtained for different T_H (= 4, 8, and 12°C) and Re (= 10, 50, 100, 150, and 200) but keeping $Ec = 0.05$. Throughout the present investigation the value of T_C has been considered to be 0°C.

The results, which are shown and discussed in the following sections, have been calculated from zero initial velocities and mean values of temperature. A grid dependence study has been carried out, as in Hossain and Wilson (2002) and Hossain and Rees (2003) for a thermally-driven cavity flow, for different values of the physical parameters, with meshes of 41 × 41, 51 × 51 and 61 × 61 points. Here also, with the aforementioned mesh points, numerical values of $\psi_{\max}$ and $\psi_{\min}$ have been calculated and entered in Table I taking into consideration that $Ra = 10.0$ and $Ec = 0.1$. From this table one can observe very small differences in the maximum or minimum values of ψ between above sets of meshes. Hence we have chosen to use 51 × 51 mesh points throughout the present computations for $\tau = 150$ with a time step of 10^{-4}, which was found to be sufficient to reach the steady-state situation for the fluid of $Pr = 11.58$ and $Gr = 10^4$. In Figure 2 we demonstrate the values of the average Nusselt number, Nu_{av}, calculated from:

$$Nu_{\text{av}} = \frac{1}{A}\int_0^A \left(\frac{\partial \theta}{\partial Y}\right)_{Y=1} \mathrm{d}X$$

along the heated surface of a rectangular cavity for $A = 2$ against τ. In this figure the graphs represents the average Nusselt number for $Ec = 0.0$, 0.5 and 1.0 while $Re = 100$.

From this figure it can be seen that the numerical values of Nu_{av} reach their respective steady values long before $\tau = 150.0$ and therefore throughout the present computations we have taken the value of $\tau = 150.0$.

Mesh points	41 × 41	51 × 51	61 × 61
$\psi_{\min}$	−6.1190	−6.0669	−5.9923
$\psi_{\max}$	0.6924	0.6713	0.6515

Table I.

Note: Numerical values of $\psi_{\min}$ and $\psi_{\max}$ for different grid points while $A = 1$, $Ra = 10.0$, and $Ec = 0.1$ at $\tau = 150$

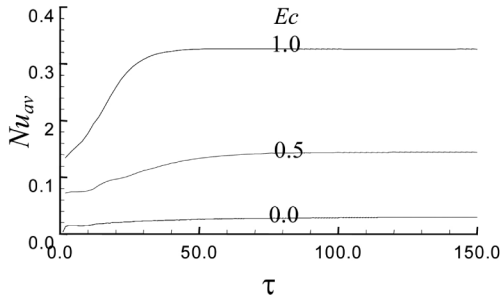

Figure 2.
Numerical values of average Nusselt number at the top moving surface for different Ec against τ while $Pr = 11.58$, $Re = 100.0$ and $T_H = 12.0$

3. Results and discussions

Investigation of a problem of unsteady, laminar, combined forced-free convection flow of water, at maximum density, in a rectangular cavity in the presence of heat due to viscous dissipation has been investigated numerically. For numerical simulation of the dimensionless equations that govern the flow we have employed the finite-difference approach along with the SOR iteration technique, considering the fact that both the vertical walls of the cavity are insulated and the top and bottom walls are maintained at different uniform temperatures. The horizontal wall at the top has been kept moving in its own plane at a constant speed while all other walls are fixed. Some representative, steady state, results are shown in Figures 3-6 for $Gr = 10^4$ and $Pr = 11.58$ in terms of streamlines and isotherms. In these figures the dotted and solid curves represent the negative and positive values of the respective functions. In case of the streamlines, the direction of the solid lines is clockwise and that of the dotted lines is counterclockwise. Here we shall term the cell with clockwise motion that is dominated by the motion of the upper surface of the cavity as the primary cell and that of counterclockwise will be termed as the secondary cell.

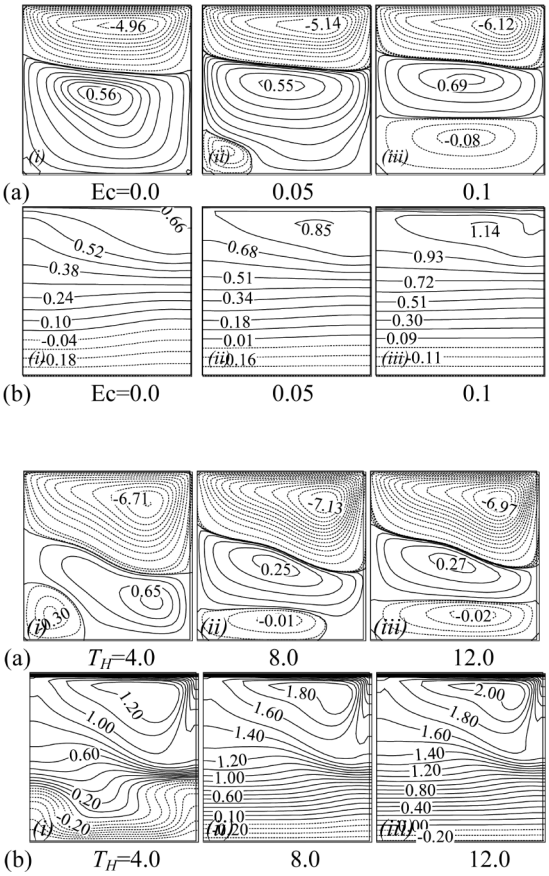

Figure 3.
Steady state (a) streamlines and (b) isotherms for different Ec while $T_H = 12.0$, $Re = 10.0$

Figure 4.
Steady state (a) streamlines and (b) isotherms for different T_H while $Ec = 0.5$, $Re = 100$

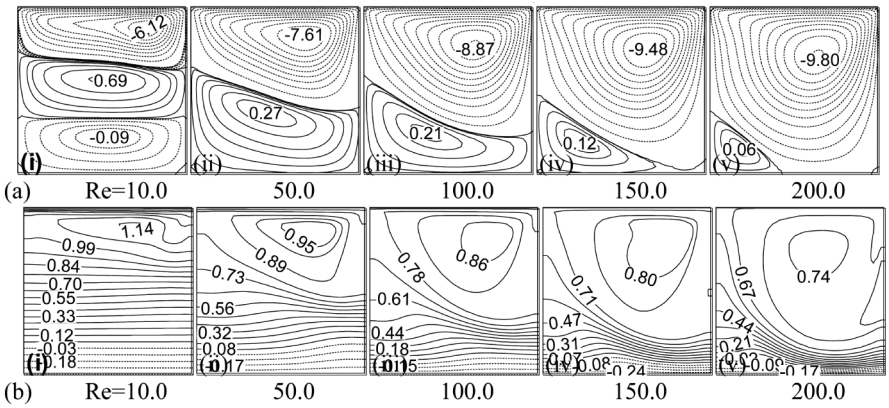

Figure 5.
Steady state (a) streamlines and (b) isotherms for different Re while $T_H = 12.0$ and $Ec = 0.05$

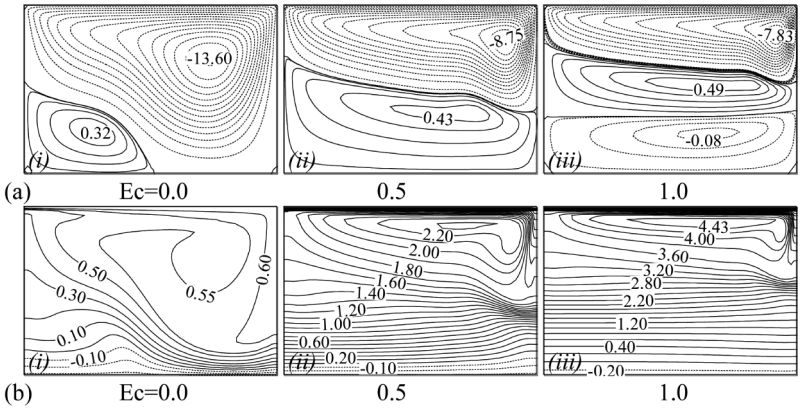

Figure 6.
Steady state (a) streamlines and (b) isotherms for different Ec while $T_H = 12.0$, $Re = 100.0$, $Pr = 11.58$, $Gr = 10^4$, and $A = 2{:}1$

We first show the effect of heat due to viscous dissipation on the streamlines by taking the value of Eckert number, Ec, as 0, 0.05 and 0.1 while the surface temperature $T_H = 12.0$ and the value of the Reynolds number, Re, is 10.0 in Figures 3a(i-iii). In Figure 3a(i) it can be seen that with the present value of Re but in absence of heat due to viscous dissipation (i.e. $Ec = 0$), there develops two vortices of opposite directions. The vortex with clockwise direction has developed along the upper surface, which is expected, since the lid is driven from the left to right. This flow is dominated by the forced flow and the center of the vortex motion is close to the upper surface and hence the intensity of the flow is higher in this region. In the lower part of the cavity the flow is counterclockwise. In this case also the vortex centre is closed to the interfacial curve that separates these vortices.

Now looking into Figures 3a(ii and iii), that are for $Ec = 0.05$ and 0.1, it can be seen that the flow rate of vortices near the upper surface increases and the centre of the vortex moves towards the right top corner of the cavity. We may further observe that

addition of heat due to viscous dissipation has forced to develop another vortex motion near the lower surface of the cavity in the direction opposite to the central one. Growing of this vortex also reduces the size as well as the flow rate in the vortex that was initially occupying the lower region of the cavity. This kind of flow is possible since addition of heat due to viscous dissipation, however small, will increase the temperature of the fluid internally that will be in support of accelerating the motion of the fluid.

The effects of heat due to viscous dissipation on the isotherms are shown in the bottom curves of Figures 3b(i-iii). From these figures it can be seen easily that the temperature of the fluid near the upper surface of the cavity increases with the increasing value of the Ec, that is expected; since in that region the rate of flow increases owing to increase of Ec as well as the rate of heat transfer from the top moving surface increases accordingly (see Figure 7a).

We see in Figures 4a(i-iii) effect of increasing T_H in a square cavity with all other parameters held fixed, and with $Re = 100$ and $Ec = 0.5$. An increase in T_H means that we have a decrease in the heat dissipation effect. Associated with that is the increasing size of the bottom left recirculation region, and that corresponds to fall in the temperature in the upper half of the cavity that is seen clearly in Figures 4b(ii-iii). When T_H is relatively small (see Figures 4(i,ii), there remains an ascending boundary layer in the bottom left corner of the cavity, since buoyancy forces are effective. Gradually this boundary layer thickness increases progressively as T_H increases and occupies the entire region near the lower surface. That is a clockwise circulation increasing in size as T_H increases. Increase of temperature near the top moving surface owing to increase in T_H is quite natural (Figures 4b(i-iii)). We further observe that at a relatively smaller value of T_H there exists a thermal boundary layer region along the cold bottom surface (Figures 4b(i)), but owing to increase in the value of T_H this layer gradually disappears and that is expected; since the rate of heat transfer from the top heated surface increases due to increase of T_H (see Figure 7).

Now we draw the attention to see the effect of increase of Reynolds number on the flow and temperature distribution in the square cavity. The streamlines and the isotherms at steady state for $Re = 10$, 50, 100, 150 and 200 are depicted, respectively, in Figures 5a(i-v) and Figures 5b(i-v) while $Ec = 0.5$ and $T_H = 12$ and keeping values of all other parameters fixed. At smaller value of Re in Figure 5a(i),

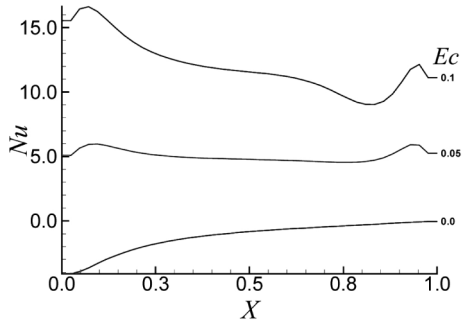

Figure 7.
Values of Nusselt number at the top moving surface for different Ec while $T_H = 12.0$, $Re = 10.0$

there exists 3-cells. With the increasing value of *Re*, the size of the primary cell adjacent to the upper moving surface gradually increases and occupies almost the entire cavity pushing down the secondary cell with anticlockwise circulation to the left bottom corner of the cavity. It is interestingly observed from the numerical computation the appearance of vortex at larger value of *Re* along the right vertical wall (although not shown here) and it is because of the presence of heat due to viscous dissipation in the flow field. Corresponding temperature distributions can be seen in Figures 5b(i-v). As before, it can be seen that increase in *Re* reduces the thermal boundary thickness near the lower cold surface and it is possible, since at larger value of *Re*, the effect of gravitation force becomes negligible. In this case the flow is governed by the forced convection and also because of increase in *Re* the rate of heat transfer form the top heated surface increases (see Figure 8).

Finally, in Figure 6a and b, we depict the streamlines and isotherms at steady state for the flow in a rectangular cavity having width $A = 2$ for three values of the viscous dissipation parameter, Ec ($= 0.0$, 0.5 and 1.0) while $T_H = 12.0$ and $Re = 100.0$. First, if we compare Figure 2a(i) with Figure 6a(i), we see that, for large aspect ratio, the primary cell that is present along the top moving surface occupies a larger space in the cavity than in case of the quire cavity, and it is because, the greater width of the cavity means that a much larger expanse of fluid due to motion of the upper surface of the cavity. As we bring the effect of heat due to viscous dissipation ($Ec = 0.5$), the size of the secondary flow that was prevailing at the left lower corner of the cavity become large and occupies almost half of the space of the cavity and this also reduces the flow rate in the primary flow region. Further increase of the heat due to viscous dissipation (when $Ec = 1.0$) separates the secondary cell from the lower cold surface and develops another cell of opposite direction. Similar flow pattern has held in case of a square cavity. From Figure 6b(i), while $Ec = 0.0$, we see that there is a thin thermal boundary layer prevails adjacent to the cold lower surface. As the effect of viscous dissipation is added and then increased, this boundary layer region disappears gradually. This is because, addition of heat due to viscous dissipation increases the temperature of the fluid in the region near the heated moving surface considerably

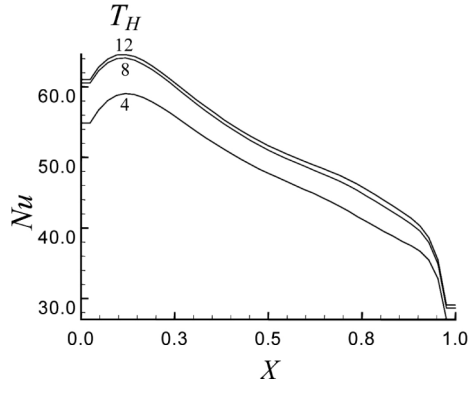

Figure 8.
Values of Nusselt number at the top moving surface for different T_H while $Ec = 0.5$, $Re = 100$

and hence results to diminish the heat transfer from the cold surface. Comparing Figures 7-10, we may conclude that the rate of increase in the heat transfer from the top heated surface is higher in case of a rectangular cavity than a square cavity.

4. Conclusions

In this paper, we have considered the problem of unsteady, laminar mixed convection heat transfer in a rectangular cavity. The vertical walls of the cavity were assumed to be insulated whereas the top and the bottom walls were maintained at two different constant temperatures. The top horizontal wall was assumed to move in its own plane at constant speed. The fluid considered was water at maximum density condition. Viscous dissipation effects were included in the analysis. The governing equations were solved numerically by the finite difference method along with SOR iteration technique.

The effect of viscous dissipation was to increase the fluid temperature and resulted in the formation of vortex motion near the lower part of the cavity in an opposite direction to the central vortex. An increase in the Eckert number and Reynolds number of the flow resulted in augmented surface heat transfer rates from the top heated surface. The results are shown for the streamlines and isotherms at various values of the Eckert number and the Reynolds number.

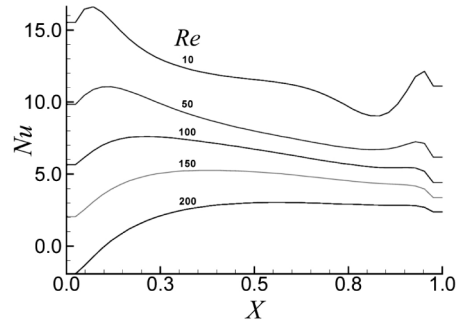

Figure 9.
Values of Nusselt number at the top moving surface for different Re while $T_H = 12.0$ and $Ec = 0.05$

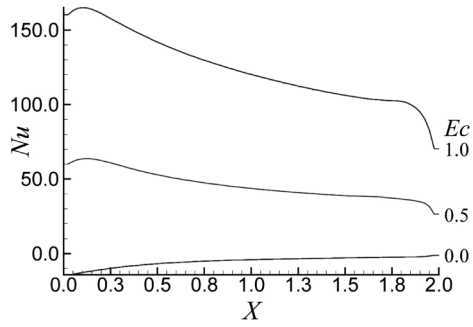

Figure 10.
Values of Nusselt number at the top moving surface for different Ec while $T_H = 12.0$, $Re = 100.0$ and $A = 2{:}1$

References

Agarwal, R.K. (1981), "A third-order-accurate upwind scheme for Navier-Stokes solutions at high Reynolds numbers", *Proc. 19th AIAA Aerospace Sciences Meeting*, AIAA-81-0112, St. Louis, MO.

Aydin, O. (1999), "Aiding and opposing mechanisms of mixed convection in a shear- and buoyancy-driven cavity", *Int. Commun. Heat Mass Transfer*, Vol. 26, pp. 1019-28.

Gebhart, B. and Mollendorf, J.C. (1977), "A new density relation for pure and saline water", *Deep Sea Res.*, Vol. 24, pp. 831-48.

Hossain, M.A. and Rees, D.A.S. (2003), "Natural convection flow of viscous incompressible fluid in a rectangular porous cavity heated from below with cold side walls", *Heat Mass Transfer*, Vol. 39, pp. 657-63.

Hossain, M.A. and Rees, D.A.S. (2004), "Natural convection flow of water near its density maximum in a rectangular enclosure having isothermal walls with heat generation", *Int Jour. Thermophysics*.

Hossain, M.A. and Wilson, M. (2002), "Natural convection flow in a fluid-saturated porous medium enclosed by non-isothermal walls with heat generation", *Int. J. Thermal Science*, Vol. 41, pp. 447-54.

Ideriah, F.J.K. (1980), "Prediction of turbulent cavity flow driven by buoyancy and shear", *J. Mech. Engng. Sci.*, Vol. 22, pp. 287-95.

Imberger, J. and Hamblin, P.F. (1982), "Dynamics of lakes, reservoirs, and cooling ponds", *Annual Rev. Fluid Mech.*, Vol. 14, pp. 153-87.

Ishikawa, M., Hirata, T. and Noda, S. (2000), "Numerical simulation of natural convection with density inversion in a squire cavity", *Numerical Heat Transfer*, Vol. 37A, pp. 195-406.

Iwatsu, R., Hyun, J.M. and Kuwahara, K. (1993), "Mixed convection in a driven cavity with a stable vertical temperature gradient", *Int. J. Heat Mass Transfer*, Vol. 36, pp. 1601-8.

Kosef, J.R. and Street, R.L. (1984), "The lid-driven cavity flow: a synthesis of qualitative and qualitative observations", *ASME J. Fluids Engng.*, Vol. 106, pp. 390-8.

Lin, D.S. and Nansteel, M.W. (1987), "Natural convection heat transfer in a square enclosure containing water near its density maximum", *Int. J. Heat Mass Transfer*, Vol. 30, pp. 2319-29.

Merker, G.P., Waas, P. and Grigull, U. (1973), "Onset of convection in horizontal water layer with maximum density effects", *Int. J. Heat Mass Transfer*, Vol. 22, pp. 505-15.

Moallemi, M.K. and Jang, K.S. (1992), "Prandtl number effects on laminar mixed convection heat transfer in a lid-driven cavity", *Int. J. Heat Mass Transfer*, Vol. 35, pp. 1881-92.

Moore, D.R. and Weiss, P. (1973), "Nonlinear penetrative convection", *J. Fluid Mechanics*, Vol. 61, pp. 553-81.

Morzynski, M. and Popiel, Cz. O. (1988), "Laminar heat transfer in a two-dimensional cavity covered by a moving wall", *Numer. Heat Transfer*, Vol. 13, pp. 265-73.

Musman, S. (1968), "Penetrative convection", *J. Fluid Mechanics*, Vol. 31, pp. 343-60.

Pilkington, L.A.B. (1969), "Review lecture: the float glass process", *Proc. Roy. Soc. London, A*, Vol. 314, pp. 1-25.

Prasad, A.K. and Kose, J.R. (1989), "Combined forced and natural convection heat transfer in a deep lid-driven cavity flow", *Heat Transfer in Convective Flows*, ASME, New York, NY, pp. 155-62, HTD-107.

Robillard, L. and Vasseur, P. (1981), "Transient natural convection heat transfer of water with maximum density effect and super cooling", *ASME J. Heat Transfer*, Vol. 103, pp. 528-34.

Schreiber, R. and Keller, H.B. (1983), "Driven cavity flows by efficient numerical techniques", *J. Comput. Phys.*, Vol. 49, pp. 310-33.

Seki, N., Fukusako, S. and Inaba, H. (1978), "Free convective heat transfer with density inversion in as confined rectangular vessel", *Heat Mass Transfer*, Vol. 11, pp. 145-56.

Thompson, M.C. and Ferziger, J.H. (1989), "An adaptive multigrid technique for the incompressible navier-stokes equations", *J. Comput. Phys.*, Vol. 82, pp. 94-121.

Tong, W. and Koster, J.N. (1993), "Natural convection of water in a rectangular cavity including density inversion", *Int. J. Heat Fluid Flow*, Vol. 14, pp. 366-75.

Torrance, K., Davis, R., Elike, K., Gill, P., Gutman, D., Hsui, A., Lyons, S. and Zien, H. (1972), "Cavity flows driven by buoyancy and shear", *J. Fluid Mech.*, Vol. 51, pp. 221-31.

Watson, A. (1972), "The effect of inversion temperature on the convection of water in an enclosed rectangular cavity", *Q. J. Mech. Appl. Math.*, Vol. 25, pp. 423-46.

Young, D.L., Liggett, J.A. and Gallagher, R.H. (1976), "Unsteady stratified circulation in a cavity", *ASCE J. the Engineering Mechanics Division*, Vol. 102 No. (EM6), pp. 1009-23.

Corresponding author
Md. Anwar Hossain can be contacted at anwar@udhaka.net